doi:10.1016/j.jmb.2007.01.088 J. Mol. Biol. (2007) 368, 8–17

JMB

Available online at www.sciencedirect.com

ScienceDirect

ELSEVIER

Haploinsuffciency for *Znf9* in *Znf9*$^{+/-}$ Mice Is Associated with Multiorgan Abnormalities Resembling Myotonic Dystrophy

Wei Chen[1,2], Yucheng Wang[1,2], Yoko Abe[1], Lukas Cheney[1] Bjarne Udd[3,4,5] and Yi-Ping Li[1,2]*

[1]*Department of Cytokine Biology, The Forsyth Institute Boston, MA 02115, USA*

[2]*Harvard School of Dental Medicine, Boston, MA 02115 USA*

[3]*Neurological Department Vaasa Central Hospital 65130 Vaasa, Finland*

[4]*Department of Neurology Tampere University Hospital and Medical School 33520 Tampere, Finland*

[5]*Folkhalsan Institute of Genetics and Department of Medical Genetics, Helsinki University Helsinki, Finland*

**Corresponding author*

Myotonic dystrophy type 2 is caused by a (CCTG)/(CCUG)$_n$ repeat expansion in the first intron of the *ZNF9* gene. The pathomechanism for the myotonic dystrophies is not well understood and the role of *ZNF9* in myotonic dystrophy type 2 pathogenesis has not been fully clarified. We characterized *Znf9*$^{+/-}$ mice, in which the expression of *Znf9* was significantly decreased, and found that their phenotype reflects many of the features of myotonic dystrophy, including muscle histological morphology, and myotonic discharges and heart conduction abnormalities, shown by electromyography and electrocardiogram analysis, respectively. *Znf9* is normally highly expressed in heart and skeletal muscle, where skeletal muscle chloride channel 1 (Clc1) plays an important role. *Clc1* expression was dramatically decreased in *Znf9*$^{+/-}$ mice. *Znf9* transgenic mice raised *Znf9* and *Clc1* expression and rescued the myotonic dystrophy phenotype in *Znf9*$^{+/-}$ mice. Our results suggest that the *Znf9* haploinsufficiency contributes to the myotonic dystrophy phenotype in *Znf9*$^{+/-}$ mice.

Keywords: *ZNF9* gene; myotonic dystrophy; *Znf9*$^{+/-}$ mice; *Znf9* haploinsufficiency; electromyography

Introduction

Myotonic dystrophy is the most common genetic muscle disease in adulthood worldwide.[1] Clinical features of myotonic dystrophy type 2 (DM2) include adult onset proximal muscle weakness, myalgic pain, myotonia, cataracts, and a whole range of possible multi-organ manifestations, such as endocrine, cardiac, serological and brain abnormalities.[2,3] Liquori *et al.* reported that the mutation responsible for DM2 is a (CCTG)/(CCUG)$_n$ repeat expansion of 75–11,000 repeats in intron 1 of the *ZNF9* gene, also referred to as *CNBP*, on chromosome 3q21.3.[4] The DM2 mutation in different populations appears to have a common founder origin.[5,6] Myotonic dystrophy type 1 (DM1) and DM2 phenotypes are strikingly similar; there are, however, distinct differences.[2,7] Mankodi *et al.* reported that DM1, caused by (CTG)/(CUG)$_n$ repeat expansions at the 3′ untranslated end of myotonic dystrophy protein kinase (*DMPK*), was reproduced in a model of *HSA*^{LR} mice expressing mRNA with CTG/CUG repeats that manifest in myotonia and the myopathic features of DM1.[8] The myotonia in *HSA*^{LR} mice is caused by the loss of skeletal muscle chloride channel 1 (Clc1) due to aberrant pre-mRNA splicing.[9,10] Mankodi *et al.* also reported that the RNA binding protein Muscleblind (Mbnl) localizes to nuclear foci of accumulated mutant RNA in myotonic dystrophy types 1 and 2.[11] Moreover, disruption of the mouse *Mbnl* gene also leads to a myotonic dystrophy disease phenotype.[12] Given the similarity of the DM1 and DM2 repeat motifs, and the fact that both expansions form nuclear mutant

Abbreviations used: DM1, DM2, myotonic dystrophy types 1 and 2; DMPK, myotonic dystrophy protein kinase; Clc1, skeletal muscle chloride channel 1; Mbnl, Muscleblind; EMG, electromyography; ECG, electrocardiogram; SCL, sinus cycle length; TG/Znf9, transgenic Znf9.

E-mail address of the corresponding author: ypli@forsyth.org

RNA foci, RNA-binding proteins that bind DM1 and DM2 expansions were suggested to mediate similar global disruptions in RNA splicing and cellular metabolism.[13–15] These findings supported the hypothesis that manifestations of DM resulted from sequestration of Mbnl by CTG/CUG or CCTG/CCUG mutant transcripts retained in the nucleus, and that the affected proteins of the splicing machinery interfered with pre-mRNA splicing regulation.[1,12,16,17] However, most recently, Mahadevan *et al.* reported that mice overexpressing a normal DMPK 3′ UTR mRNA reproduced cardinal features of myotonic dystrophy, including myotonia, cardiac conduction abnormalities, histopathology and RNA splicing defects in the absence of detectable nuclear inclusions.[18] They also found increased levels of CUG-binding protein in skeletal muscle, common to DM1 patients, and that in transgenic mice expressing the wild-type DMPK 3′ UTR with $(CTG)_5$, the short CTG/CUG repeats were sufficient to cause DM1 pathology without RNA or Mbnl foci.[18]

Although DM1 and DM2 phenotypes are largely similar clinical syndromes, they are not identical.[19] DM2 usually has a more benign disease course than DM1; i.e. dysphagia and respiratory failure do not occur at later stages of the disease. DM2 does not show any congenital form, and the considerable central nervous system involvement in DM1 is not obvious in DM2.[2] Muscle pathology is also different in DM2 compared to DM1.[20] Together, these dissimilarities indicate differences in which genes are secondarily affected and also how and when they are affected by the repeat expansions in DM1 and DM2. The differences between DM2 and DM1 cannot be explained by the previous theory of DM pathology. It is still not known whether the entire disease pathology of DM1 and DM2 is caused by interference in RNA processing.[19] The results of Mahadevan *et al*., together with the finding that RNA foci formation and splicing defects are separable,[21] highlight the need to re-examine myotonic dystrophy pathogenesis. Based on these controversial results, as well as on the unexplained role of *Znf9*/*ZNF9* in the regulation of muscle gene expression,[22] we wanted to know if deficiency of Znf9 protein might have a pathogenic effect similar to DM2.

Results

Changes similar to the myotonic dystrophy phenotype in *Znf9*$^{+/-}$ mice

We characterized 80 *Znf9*$^{+/-}$ mice in the C57BL/6J background and found that 80% of *Znf9*$^{+/-}$ mice showed a phenotype with multi-organ changes associated with myotonic dystrophy at two to six months of age. Our previous work has demonstrated that the retrovirus insertion mutagenesis in *Znf9* (Figure 1(a) and (b)) resulted in null mutation *Znf9*$^{-/-}$ in homozygous embryos, which had severe forebrain truncation and died around E10.5.[23] Here, we characterized the *Znf9*$^{+/-}$ mouse phenotype and its defects. We observed many abnormalities of myotonic dystrophy expressed in the *Znf9*$^{+/-}$ phenotype, including myotonia, ocular cataracts, cardiac arrhythmia, and both proximal and distal muscle wasting (Figure 1(c) to (l) and Figure 2). *Znf9*$^{+/-}$ mice displayed defective walking and could not make clear footprints when compared with wild-type mice (Figure 1(c) and (d)). *Znf9*$^{+/-}$ mice could not hold up their bodies and fell down within 3 s while wild-type mice could hold up their bodies longer than 15 s (Figure 1(e) and (f)).

In addition to muscle abnormalities, ocular cataracts that progress from posterior sub-capsular iridescent opacities to mature cataracts is a prominent DM-associated feature.[4] Such cataracts were observed in 25% of the *Znf9*$^{+/-}$ eyes examined ($n=36$; 6 to 12 months old; Figure 1(h) to (j)), but in none of their wild-type siblings (Figure 1(g)). In DM2, cardiac arrhythmia is a major cause of death.[24] The hearts were 50% enlarged in 75% of *Znf9*$^{+/-}$ mice examined, as compared with those in wild-type mice (Figure 1(k)), and the walls of the heart chambers were thickened by 1.5-fold (Figure 1(l)), which is suggestive of a hypertrophic cardiomyopathy heart defect in *Znf9*$^{+/-}$ mice. Hypertrophic cardiomyopathy is not a constant finding in human patients but has occasionally been reported in DM2.[25]

To further characterize the phenotype of *Znf9*$^{+/-}$ mice, we examined the histology of skeletal and heart muscle from two to six-month-old wild-type and *Znf9*$^{+/-}$ mice. Hematoxylin and eosin staining showed that *Znf9*$^{+/-}$ mice had more than twice the number of nuclei per skeletal muscle fiber, a much higher proportion of central nuclei, and increased variability in fiber size, all relative to wild-type mice (Figure 2(a) to (d)). Heart muscle histology of *Znf9*$^{+/-}$ mice showed the same pathology mentioned in skeletal muscle when compared with wild-type (Figure 2(e) to (h)). In human DM2, there is a similar marked increase in central nuclei as was noted in *Znf9*$^{+/-}$ mice (Figure 2).[2,20] Heart tissues of *Znf9*$^{+/-}$ mice also showed myocardial hypertrophy and fibrosis as compared to those of wild-type mice (Figure 2(e) to (h)). The myocardial hypertrophy and fibrosis may reflect cardiomyopathy, affect heart function, and cause death, as observed for *Znf9*$^{+/-}$ mice, about 25% of which die within the first half-year.

Myotonic discharges in *Znf9*$^{+/-}$ mice revealed through electromyography (EMG) and heart conduction abnormalities on electrocardiogram (ECG)

Myotonia is a prominent feature of myotonic dystrophy. Myotonic discharges were revealed, through EMG of vastus muscle, in 80% of the *Znf9*$^{+/-}$ muscle ($n=60$) in contrast to normal EMG electrode insertional activity in wild-type muscle (Figure 3(a) and (b)). Seventy-five percent of the *Znf9*$^{+/-}$ mice were found to have abundant myotonia in all muscles examined, with variable-frequency

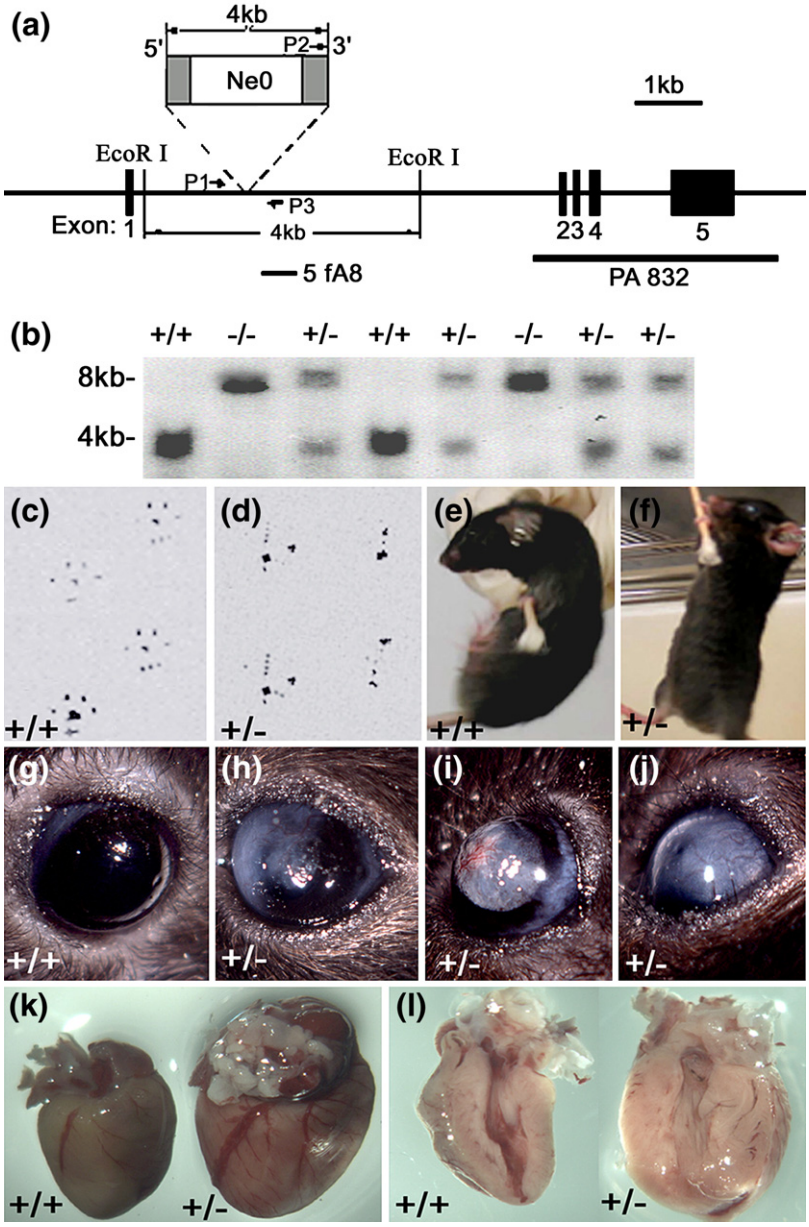

Figure 1. The phenotype of *Znf9*$^{+/-}$ mouse morphology reflects myotonic dystrophy. (a) The integration site of the provirus in the *Znf9* gene locus. (b) Genotype analysis of *Znf9*$^{+/-}$ mutant mice by Southern blot. (c) and (d) *Znf9*$^{+/-}$ mice (d) exhibit defective walking and cannot make clear footprints, which may be attributed to muscle weakness, when compared with wild-type mice (c). (e) and (f) Muscle weakness develops in *Znf9*$^{+/-}$ mice (f) when compared with wild-type mice (e). *Znf9*$^{+/-}$ mice (f) cannot hold up their bodies and fall down within 3 s. (g)–(j) Distinctive ocular cataracts that progressed from posterior sub-capsular "dust-like" opacities to mature cataracts are observed in 25% of *Znf9*$^{+/-}$ eyes examined ($n=36$; 6 to 12 months old; (h) to (j) but not in wild-type siblings (g). (k) Heart hypertrophy of mutant heart is observed and the heart is enlarged in *Znf9*$^{+/-}$ mice when compared with that in wild-type mice. (l) The walls of the heart chambers in *Znf9*$^{+/-}$ mice are thicker when compared with those in wild-type mice.

(50 to 200 Hz) runs of muscle action potentials that continued for 60 s after insertion or repositioning of the recording electrode (Figure 3(b)). These repetitive discharges were present in *Znf9*$^{+/-}$ mice as early as three weeks of age, indicating that *Znf9*$^{+/-}$ mice had a true myotonic disorder, rather than nonspecific hyperexcitability associated with muscle fiber lesions.

The primary clinical cardiac manifestation in DM2 is the development of conduction disturbances, with arrhythmia, progressive atrioventricular (A–V) block and bradycardia.[26] To assess the effects of *Znf9* dosage alterations on heart function, ECG analysis was obtained on mature *Znf9*$^{+/-}$ mice ($n=30$) and wild-type control mice ($n=15$) at six to seven months. Cardiac arrhythmia (Figure 3(d)) and significantly prolonged mean P–R duration (first-degree A-V block) was discovered in 80% of *Znf9*$^{+/-}$ mice as compared with wild-type mice (Figure 3(c)). A 105 ms sinus cycle length (SCL) and a 30 ms P–R interval were displayed in the control wild-type mouse (Figure 3(e)). ECG results showed a prolonged P–R interval, an SCL of 113 ms, and a P–R interval of 42 ms in 80% of *Znf9*$^{+/-}$ mice (Figure 3(f)). These results demonstrated that *Znf9* dosage was a critical element modulating cardiac conduction integrity and apparently linked haploinsufficiency of *Znf9* with conduction abnormality in *Znf9*$^{+/-}$ mice.

Znf9 expression pattern of *Znf9*$^{+/+}$ and *Znf9*$^{+/-}$ mice

To clarify the role of *Znf9* in muscle and heart functions, we analyzed the expression of Znf9/*Znf9* in the heart and skeletal muscle of newborn mice using immunostaining, *in situ* hybridization, and Northern blot. Immunostaining revealed that the *Znf9* was expressed in the skeletal (Figure 4(a) and (b)) and heart muscle (Figure 4(d) and (e)). The

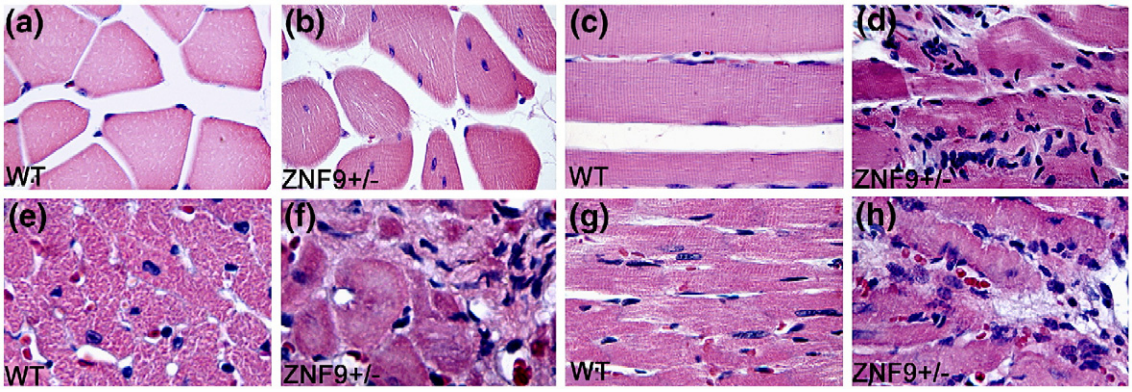

Figure 2. The skeletal and heart muscle phenotype of *Znf9*$^{+/-}$ mice reflects myotonic dystrophy. (a)–(d) Skeletal muscle histology analysis of wild-type (WT) and *Znf9*$^{+/-}$ mice through hematoxylin and eosin staining. Representative images are transverse frozen sections of vastus muscle ((a) and (b)) and vertical frozen sections of vastus muscle ((c) and (d)) obtained from six-month-old mice. Hematoxylin and eosin-stained muscles show increased central and peripheral muscle nuclei and increased variability in the muscle of mutant *Znf9*$^{+/-}$ mice ((b) and (d)) as compared with that of wild-type mice ((a) and (c)). (e)–(h) Heart muscle histology analysis of wild-type and *Znf9*$^{+/-}$ mice. Heart muscle in *Znf9*$^{+/-}$ mice ((f) and (h)) shows increased central and peripheral muscle nuclei and severe fibrosis compared to wild-type mice ((e) and (g)). These results are representative of four separate experiments in *Znf9*$^{+/-}$ line and two experiments in wild-type lines.

expression in muscle was confirmed at the mRNA level by *in situ* hybridization (Figure 4(g) and (h)). No signal was detectable when normal serum and sense probes were used (Figure 4(c), (f), and (i)). We detected *Znf9* expression in the developing heart of mice embryos at E10 using whole mount *in situ* hybridization (Figure 4(j)), suggesting that *Znf9* plays a role in heart development during embryonic stages. Northern blot showed that, although *Znf9* is broadly expressed in many tissues, the highest expression is in heart and skeletal muscle (Figure 4(k) and (l)), the two tissues predominantly affected in DM2. As expected, *Znf9* expression significantly decreased in heterozygous mutant *Znf9*$^{+/-}$ mouse skeletal and heart muscle (Figure 4(m) and (n)).

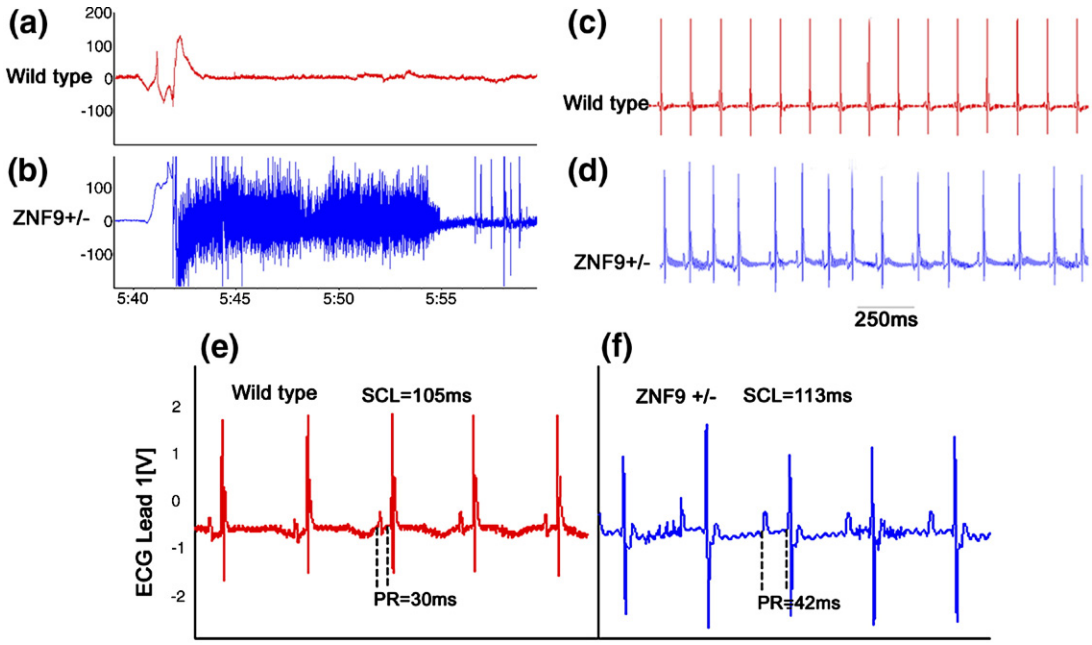

Figure 3. Myotonic discharges and heart conduction abnormalities in *Znf9*$^{+/-}$ mice. (a) and (b) EMG recordings in skeletal muscle of mice from wild-type and *Znf9*$^{+/-}$ lines elicited by brief movement of the EMG electrode. In wild-type mice (a), no myotonic discharge is observed after insertion or repositioning of the recording electrode. In *Znf9*$^{+/-}$ mice (b), EMG reveals high-frequency runs of muscle action potentials that continue for more than 60 s after insertion or repositioning of the recording electrode. (c) and (d) ECG reveals cardiac arrhythmia of *Znf9*$^{+/-}$ mice (d) compared with wild-type mice (c). (e) A control wild-type mouse has an SCL of 105 ms and a P–R interval of 30 ms. (f) ECG shows prolonged P–R interval in the *Znf9*$^{+/-}$ mouse, with an SCL of 113 ms and a P–R interval of 42 ms. The mean P–R interval is significantly longer in heterozygous adult mice, compared with control mice. $N = 15$.

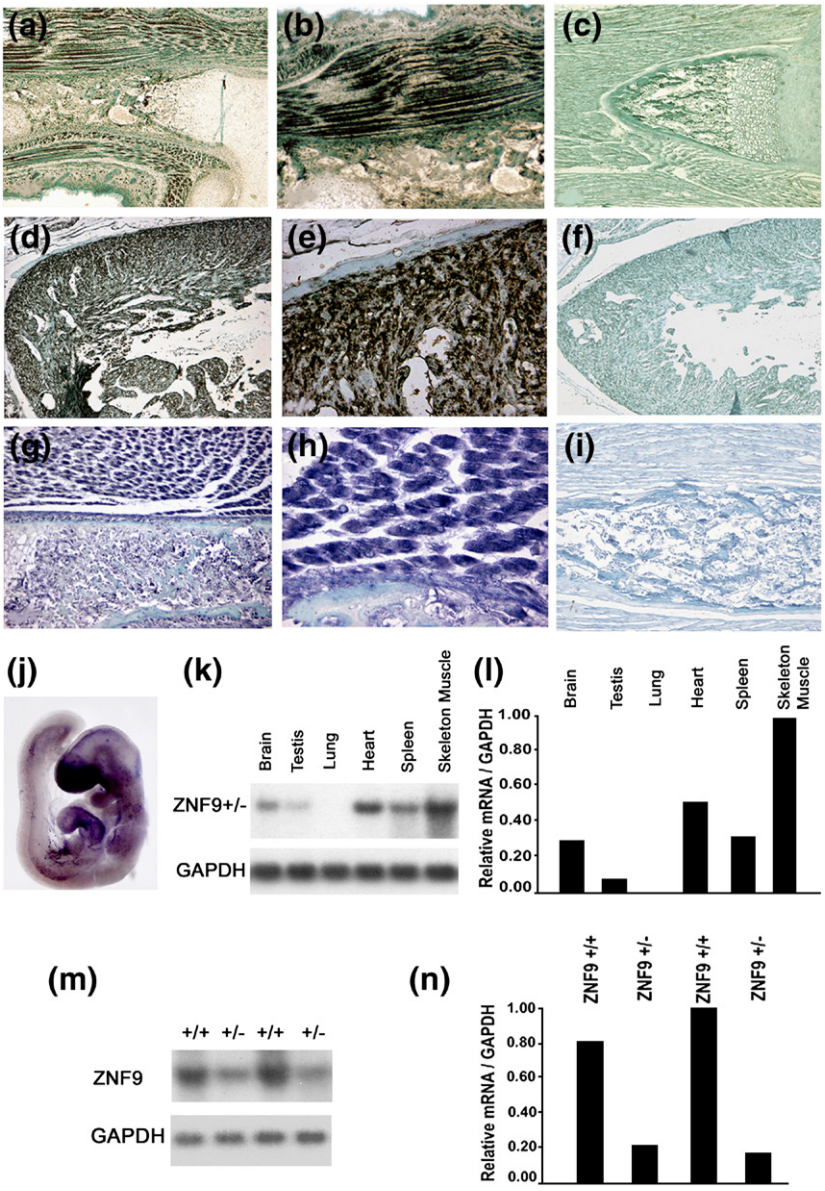

Figure 4. *Znf9* expression in muscle and heart in wild-type mice and embryos. (a)–(c) Skeletal muscle immunohistochemistry. (a) Znf9 protein is detected in skeletal muscle using anti-Znf9 antibody. (b) The amplification of (a). (c) Normal serums from wild-type mice were used as negative controls. (d)–(f) Heart muscle immunohistochemistry. (d) The Znf9 protein is detected in heart using anti-Znf9 antibody. (e) The amplification of (d). (f) Normal serums from wild-type mice were used as negative controls. (g)–(i) *In situ* hybridization of the mRNA level. (g) *Znf9* mRNA is detected using *Znf9* antisense as a probe. (h) The amplification of (g). (i) *Znf9* sense from wild-type mice was used as negative control. (j) Whole mount *in situ* hybridization of E10.5 mouse embryo. Besides expression of *Znf9* in forebrain and limb bud that is described, *Znf9* is detected in the developing heart. (k) Analysis of *Znf9* mouse tissue distribution by Northern blot. *Znf9* is broadly expressed, with the highest expression in heart and skeletal muscle, two tissues predominantly affected in DM2. (l) The results of (k) were normalized for GAPDH, and are presented as relative units. $N = 5$. (m) In the heterozygous state there is a significant reduction of *Znf9* expression both in heart (lane 2) and in skeletal muscle (lane 4) as compared with that of wild-type (lanes 1 and 3). (n) The results of (m) were normalized for GAPDH, and are presented as relative units. $N = 5$.

Znf9 transgenic mice rescue the myotonic dystrophy phenotype in *Znf9*$^{+/-}$ mice

The retrovirus insertion in the first intron of *Znf9* could also result in the expression defect of the genes flanking *Znf9*. To prove *Znf9* haploinsufficiency is the only factor that causes myotonia, we carried out *Znf9* overexpression experiments using three *Znf9* transgenic (*TG/Znf9*) lines. A schematic illustrates the *Znf9* transgene-containing 10 kb mouse *Znf9* promoter, 11 kb entire *Znf9* gene, and 300 bp vector DNA sequence as a tag for genotyping (Figure 5(a)). Transgenic genotyping by PCR was analyzed using primers P1 and P2 (Figure 5(b)). Northern blot showed that weakly expressed *Znf9* in *Znf9*$^{+/-}$ mutants was expressed at high levels in *TG/Znf9*$^{+/-}$ mice compared with wild-type mice (Figure 5(c) and (d)). Interestingly, *TG/Znf9*$^{+/-}$ mice showed no phenotype and did not develop histologically defined myopathy. *Znf9*$^{+/-}$ mutants showed defects in skeletal (Figure 6(a) and (c)) and heart muscle (Figure 6(e) and (g)), while transgenic-rescued *TG/Znf9*$^{+/-}$ mice (Figure 6(b), (d), (f), and (h)) were normal. Myotonic discharges, cardiac arrhythmia, and A–V conduction abnormalities shown in *Znf9*$^{+/-}$ mutants were completely rescued in *TG/Znf9*$^{+/-}$ mice (Figure 7(a) to (i)). These results suggested that *Znf9* overexpression had the ability to rescue the pathology in both skeletal and heart muscle of the *Znf9*$^{+/-}$ mutants. The same result was obtained from all three transgenic lines.

Haploinsufficiency of *Znf9* causes a decrease in the amount of *Clc1* mRNA

We wondered whether haploinsufficiency of *Znf9* might cause the decrease in the amount of *Clc1* mRNA that would cause the myotonia. Semi-quantitative RT-PCR was conducted on equal amounts of RNA extracted from skeletal muscle of

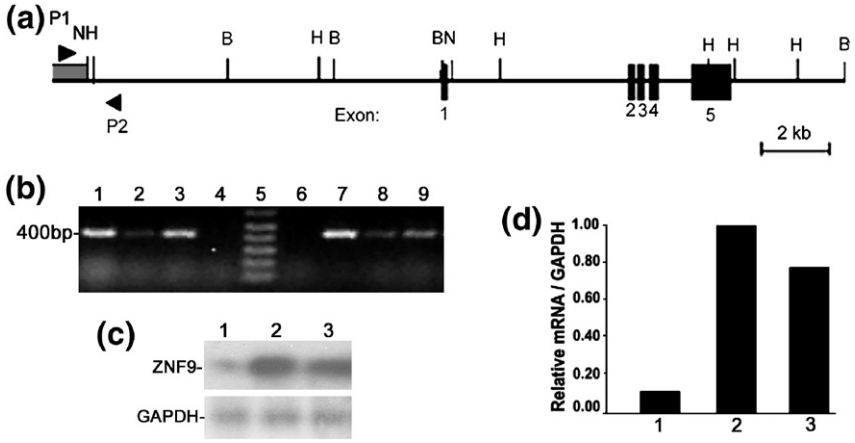

Figure 5. *Znf9* transgene construct, genotype, and rescue of *Znf9* expression in *Znf9*$^{+/-}$ mice. (a) Diagram of the *Znf9* construct, showing the *Znf9* transgene containing a 10 kb mouse *Znf9* promoter, 11 kb entire *Znf9* gene, and a 300 bp vector DNA sequence as a tag for genotyping. Filled boxes are the *Znf9* sequences of five exons. (b) Transgenic genotyping by PCR analysis using primers P1 and P2. Lanes 4 and 6 are control DNA from wild-type mice. Lane 5 is a DNA marker. A 400 bp fragment represents recovery of transgenic embryos. (c) *Znf9* expression rescued by transgenic mice. Lane 1 shows muscle *Znf9* expression in the *Znf9*$^{+/-}$ mutant. *Znf9* expression is dramatically reduced compared with that in wild-type mice (lane 3). *Znf9* is highly expressed in *TG/Znf9*$^{+/-}$ mice (lane 2). (d) The results of (c) were normalized for GAPDH, and are presented as relative units. $N=5$.

wild-type, *Znf9*$^{+/-}$ mutant, and *TG/Znf9*$^{+/-}$ transgenic mice. The result showed that in *Znf9*$^{+/-}$ mutant mice, the amount of *Clc1* mRNA was dramatically decreased compared to that of the wild-type mice. Most interestingly, in *TG/Znf9*$^{+/-}$ mice, the amount of *Clc1* mRNA was even higher than in wild-type mice (Figure 8(a) and (b)). To further confirm the result of semi-quantitative RT-PCR, we conducted Northern blot analysis of *Clc1* level in skeletal muscle of wild-type, *Znf9*$^{+/-}$ mutant, and *TG/Znf9*$^{+/-}$ mice. Mouse cDNA fragments spanning from exon 4 to exon 8 were used as probes to analyze *Clc1* expression. There was a significant reduction in *Clc1* mRNA in *Znf9*$^{+/-}$ mutant muscle and the *TG/Znf9*$^{+/-}$ transgene rescued the decreased amount of *Clc1* mRNA in *Znf9*$^{+/-}$ mutant muscle. The Northern blot result further confirmed that the *TG/Znf9* transgenic mice rescued the low *Clc1* expression in *Znf9*$^{+/-}$ mutant muscle (Figure 8(c) and (d)). Taken together these results suggest that low levels of *Znf9*, as described here for the mouse model, result in low levels of *Clc1* expression and apparent myotonia and that *Clc1* expression might be regulated by *Znf9*.

Discussion

Possible DM1/2 mechanisms include: (i) pathogenic effects of the $(CUG)/(CCUG)_n$ RNA expansion that disrupts cellular function[13–15] as described in the pathogenesis of DM1,[8–12] irrespective of its accumulation as nuclear foci,[1,27] and was to some extent confirmed in DM2;[28] (ii) aberrant RNA splicing of other genes caused by sequestered or altered amount of splicing machinery proteins by mutant RNA; and (iii) altered expression of mutated and neighboring genes as described in DM1.[29,30] However, our data show that Znf9 cannot be excluded from playing a role in DM2 since haploinsufficiency of *Znf9* in the *Znf9*$^{+/-}$ mutant mice generated by retrovirus insertion in intron 1 of *Znf9*,[23] instead of the $(CCTG)/(CCUG)_n$ expansion, reproduces multi-organ abnormalities associated

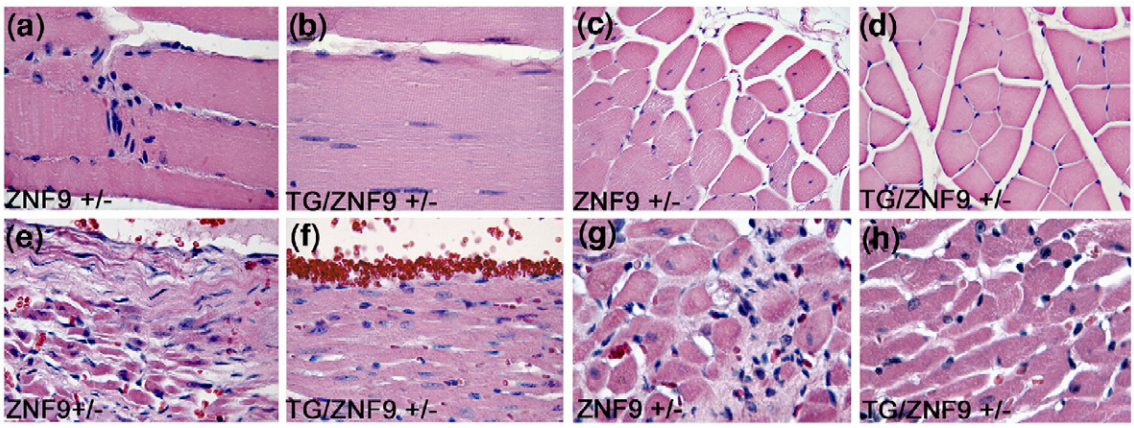

Figure 6. The *Znf9* transgene rescued the phenotype defects of *Znf9*$^{+/-}$ mouse skeletal and heart muscle. (a)–(d) Skeletal muscle in the *Znf9*$^{+/-}$ mutant ((a) and (c)) shows the same defects described in Figure 2, while skeletal muscle of transgenic *TG/Znf9*$^{+/-}$ mice ((b) and (d)) is normal. (e)–(h) Heart muscle in the *Znf9*$^{+/-}$ mutant ((e) and (g)) shows the same defects described in Figure 2, while heart muscle of transgenic *TG/Znf9*$^{+/-}$ mice ((f) and (h)) is normal.

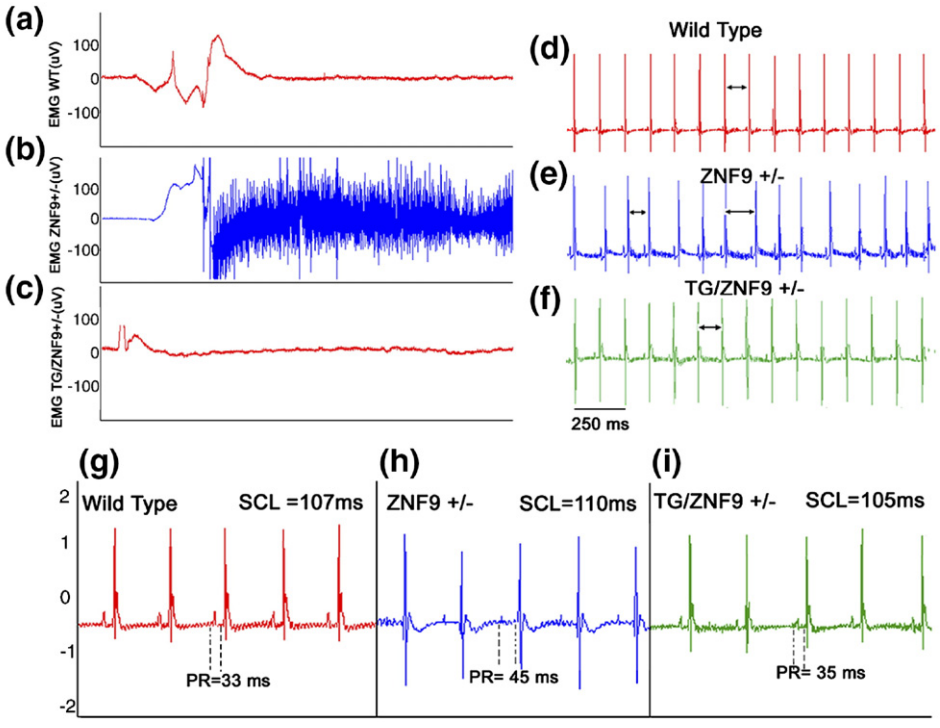

Figure 7. The *Znf9* transgene rescued the altered functions of *Znf9*$^{+/-}$ mouse skeletal and heart muscle. (a)–(c) EMG recordings in skeletal muscle of mice from wild-type (a), *Znf9*$^{+/-}$ (b), and *TG/Znf9*$^{+/-}$ lines (c), elicited by brief movement of the EMG electrode, indicating that the myotonia phenotype has been rescued. (d)–(f) ECG from wild-type (d), *Znf9*$^{+/-}$ (e), and *TG/Znf9*$^{+/-}$ (f) mice shows cardiac arrhythmia is rescued in *TG/Znf9*$^{+/-}$ mice. (g)–(i) A control wild-type mouse (g) has an SCL of 107 ms and a P–R interval of 33 ms. ECG shows a prolonged P–R interval in the *Znf9*$^{+/-}$ mouse (h), with a SCL of 110 ms and a P–R interval of 45 ms. A recording from a *TG/Znf9*$^{+/-}$ mouse (i), with a SCL of 105 ms and a P–R interval of 35 ms shows that A–V conduction abnormalities are rescued. $N = 5$.

with myotonic dystrophies. The working model holding that manifestations of DM result from sequestration of Mbnl by CTG/CUG or CCTG/CCUG mutant transcripts retained in the nucleus, and that the affected proteins of the splicing machinery interfere with pre-mRNA splicing regulation,[1,12,16,17] had been widely accepted. However, Mahadevan *et al.*'s finding that overexpression of normal DMPK 3′ UTR mRNA causes increased CUG-binding protein and myotonic dystrophy

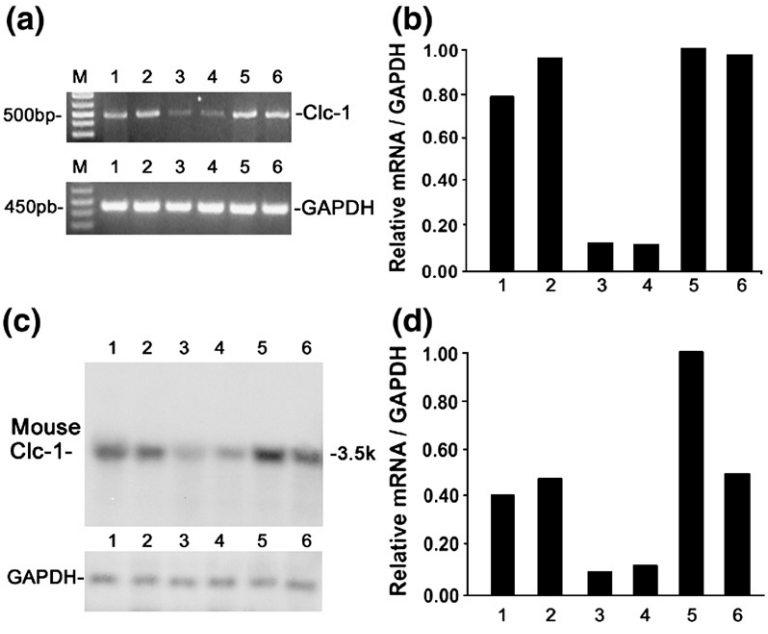

Figure 8. Semi-quantitative RT-PCR and Northern blot analysis of the *Znf9* level. (a) Semi-quantitative RT-PCR of the *Clc1* mRNA in wild-type (lanes 1 and 2), *Znf9*$^{+/-}$ mutant (lanes 3 and 4), and *TG/Znf9*$^{+/-}$ (lanes 5 and 6) skeletal muscle. The results revealed that the amount of *Clc1* mRNA was reduced in *Znf9*$^{+/-}$ mutant muscle and that the *TG/Znf9*$^{+/-}$ transgene rescued the decreased amount of *Clc1* mRNA in *Znf9*$^{+/-}$ mutant muscle. (b) The results of (a) were normalized for GAPDH, and are presented as relative units. (c) Analysis of the *Clc1* level by Northern blot. The *Clc1* mRNA in wild-type (lanes 1 and 2), *Znf9*$^{+/-}$ mutant (lanes 3 and 4), and *TG/Znf9*$^{+/-}$ (lanes 5 and 6) skeletal muscle. The same results were found as in (a). (d) The results of (c) were normalized for GAPDH, and are presented as relative units. $N = 5$.

without Mbnl-containing ribonuclear inclusions[18] is not a straightforward fit with previous theory, indicating that there are still open issues in the pathomechanism of myotonic dystrophies.

Mahadevan *et al*. concluded that a conundrum remains in the explanation of DM pathology; it is still not clear why mice overexpressing a normal *DMPK* 3′ UTR develop the disease.[18] They suggested that the effects of overexpression of many *DMPK* 3′ UTR transcripts with $(CUG)_5$ in mice may be pathogenically equivalent to expressing mutant transcripts with hundreds of CTG/CUG repeats.[18] However, this could not explain the normal phenotype of transgenic mice with short CTG/CUG repeats found by Mankodi *et al.*[8] They stated that the sequence elements required for toxicity and that induce higher CUG-binding protein levels exist within the normal transcript.[18]

We aimed to help clarify the conundrum pointed out by Mahadevan *et al.* through our study of *Znf9*. Based on our work we propose that the *Znf9* haploinsufficiency contributes to the myotonic dystrophy phenotype in *Znf9*$^{+/-}$ mice. Our results showing many abnormalities of myotonic dystrophy expressed in the *Znf9*$^{+/-}$ phenotype, including myotonia, ocular cataracts, cardiac arrhythmia, and muscle wasting, along with myotonic discharges and heart conduction abnormalities, provide strong evidence that *Znf9* is involved in DM pathology. Notably, the myotonic dystrophy phenotype in *Znf9*$^{+/-}$ mice can be fully rescued by the *TG/Znf9*$^{+/-}$ transgene, which also means that altered expression of neighboring genes is less likely to be of importance for pathogenesis. These effects were reversible in both mature skeletal and cardiac muscles by silencing transgene expression. Our results may also suggest a possible therapeutic strategy for treatment by increasing *ZNF9* expression.

Currently we do not know how haploinsufficiency causes the myotonic dystrophy phenotype in *Znf9*$^{+/-}$ mice. However, our data do show that *Znf9* is important in the normal function of skeletal and cardiac muscle. Decreased expression of *Clc1* in *Znf9*$^{+/-}$ mice may give an important clue to further explore the mechanism that causes the DM2-like phenotype in *Znf9*$^{+/-}$ mice. Aberrant splicing leading to low expression of functional Clc1 is considered the major pathogenetic mechanism of myotonia in myotonic dystrophy.[10] *Clc1* was significantly decreased in *Znf9*$^{+/-}$ mice, which showed definite myotonia. The decrease in *Clc1* could result from decreased expression at the transcriptional level or could be caused by aberrant splicing. We did not, however, find evidence of aberrant splicing of *Clc1*. We suspect that Znf9 regulates *Clc1* expression at the transcriptional level. Konicek *et al.* found that AP1 and CNBP (Znf9) bind to the promoter of M-CSF and regulate its expression.[31] We performed a search for Znf9 conserved binding sites that show 90% similarity with that in the promoter of M-CSF within the region flanking the 5′ end of the *Clc1* promoter and found two sites in the first 100 bp (data not shown), indicating that Znf9 could regulate *Clc1*. It remains to be confirmed, however, whether Znf9 does regulate *Clc1* expression and further study is needed to categorize the cause of low *Clc1* expression in our mouse model.

In this study the *Znf9*$^{+/-}$ knock-out allele was not fully penetrant. The *Znf9*$^{-/-}$ was fully penetrant, with all embryos dying around E10.5.[23] It is common to find reduced penetrance of heterozygous knock-outs, in which the expression of the gene is variable. This could be caused by genetic variations in each individual mouse. We have previously found that the expression of *Znf9* in the heterozygous knock-out, while consistently lower than in the wild-type, varied among individuals.[23]

Our *Znf9*$^{+/-}$ mice showed both proximal and distal muscle wasting, while proximal muscle wasting is predominant in DM2 patients. We suspect that this is due to the species differences between humans and mice and the underlying difference in primary gene defect. The established pathogenetic mechanism in DM2 and DM1, aberrant splicing of a large set of genes, is thought to be based on similar mechanisms in both diseases, and still, the molecular basis for the opposite muscle wasting phenotype in DM2 *versus* DM1 is unexplained. Our *Znf9*$^{+/-}$ mice may have secondary target genes that are in common with those affected in both DM1 and DM2.

Znf9$^{+/-}$ mice show some features of the DM2 phenotype and it is possible that *Znf9*$^{+/-}$ mutants could be used as a DM2 or myotonic dystrophy mouse model. Extensive further study is needed to define the role of ZNF9 in the pathogenesis of human myotonic dystrophy type 2. The proposed importance of *Znf9* haploinsufficiency for the DM phenotype in *Znf9*$^{+/-}$ mice indicates that, if directly transferred to the human DM2 situation, nonsense mutations in *ZNF9* would replicate the pathology observed here in *Znf9*$^{+/-}$ mice. To date, *ZNF9* nonsense or missense mutations in the tested DM2 population have not yet been observed. Moreover, the total amount of ZNF9 protein in one DM2 patient muscle sample was recently reported not to be decreased.[32] However, the previous studies only present data for total levels of ZNF9. An important extension of our study would be to investigate the activity and intracellular distribution of ZNF9 in DM patients, which could reveal a mechanistic link between DM and ZNF9. Also, the regulatory effects of Znf9 in mice may be very different from those of ZNF9 in humans.

In the interest of myotonic dystrophy research, adding further relevant data to the complexity of myotonic dystrophy pathogenesis is of general interest. The next steps in the evaluation of our mouse model will include studies on processing and sub-cellular localization of Znf9 isoforms and expression data on the different genes shown to be aberrantly spliced in myotonic dystrophies, in order to understand where the molecular paths of Znf9 haploinsufficiency and of $(CCTG)/(CCUG)_n$ repeat expansion pathomechanisms may cross each other.

Materials and Methods

Znf9$^{+/-}$ mutant mouse strain and genotype

The Znf9 mutant mouse strain, also termed Znf9$^{+/-}$ mutant mouse strain, was generated and genotyped as described.[23] The Znf9$^{+/-}$ mutants were repeatedly backcrossed for 15 generations with the C57BL/6J inbred genetic background to improve phenotypic consistency.

RNA preparation and analysis

RNA preparation and analysis was performed as described.[33] Full-length mouse Znf9 cDNA fragments were used as probes to analyze Znf9 expression. Mouse cDNA fragments spanning from exon 4 to exon 8 were used as probes to analyze Clc1 expression. The results shown were reproduced at least four times.

Analyses of histology, immunostaining, and *in situ* hybridization

These techniques were performed as described.[23] All the results shown were reproduced at least four times. All hybridization results were normalized against the GAPDH signal.

Transgenic rescue of DM2 phenotypes in *Znf9*$^{+/-}$ mutants

Znf9 transgenic mice were used to rescue DM2 phenotypes of *Znf9*$^{+/-}$ mutants as described.[23] In brief, transgenic (*TG*) mice were crossed to *Znf9*$^{+/-}$ mutants, and the resultant progeny (*TG/Znf9*$^{+/-}$) were backcrossed to *Znf9*$^{+/-}$ mice.

Electrocardiography and electrophysiology studies

The mouse electrophysiological study methodology has been described in detail.[34,35] Cardiac rhythm and respirations were monitored, ECG intervals calculated, and standard pacing protocols used to determine the electrophysiologic parameters.[34–36] All the results shown were reproduced at least four times.

Data acquisition and analysis

Surface ECGs and electrogram recordings were acquired on a multi-channel amplifier and converted to a digital signal for analysis (MacLab System, AD Instruments, Milford, MA).

Semi-quantitative RT-PCR

For mouse E4-E8, the upstream primer (5′- ATGAAGCCTAGCCTTCCTCT –3′) and downstream primer (5′- ATCCTTGTTCCAAACGGCCA –3′) were used. After the first strand cDNA was synthesized, amplification was performed using 25 cycles of 30 s at 95 °C, 30 s at 60 °C, and 30 s at 72 °C, followed by a final 10 min extension at 72 °C. GAPDH was used as a quantitative control. The results shown were reproduced at least four times.

Statistical analysis

All continuous variables, such as ECG intervals and cardiac conduction properties, were compared to gender and age-matched controls, with data presented as the mean±1 standard deviation. Statistical analysis includes the 2-tailed Student's *t* test, analysis of variance (ANOVA) with Scheffé subgroup testing when appropriate, and analysis of inter-observer variability. A P value of <0.05 is considered statistically significant.

Acknowledgements

We thank Ms Carrie Soltanoff for her excellent assistance with the manuscript. We think Mr Ming Li for his technical assistance. This work was supported by NIH grant AR-44741 (to Y.-P. L.) and AR-48133 (to Y.-P. L.), and by grants from the Liv & Halsa Foundation and Vasa Hospital Region Medical Research Foundation (to B.U.).

References

1. Tapscott, S. J. (2000). Deconstructing myotonic dystrophy. *Science*, **289**, 1701–1702.
2. Day, J. W., Ricker, K., Jacobsen, J. F., Rasmussen, L. J., Dick, K. A., Kress, W. *et al.* (2003). Myotonic dystrophy type 2: molecular, diagnostic and clinical spectrum. *Neurology*, **60**, 657–664.
3. Ricker, K., Koch, M. C., Lehmann-Horn, F., Pongratz, D., Otto, M., Heine, R. & Moxley, R. T., 3rd (1994). Proximal myotonic myopathy: a new dominant disorder with myotonia, muscle weakness, and cataracts. *Neurology*, **44**, 1448–1452.
4. Liquori, C. L., Ricker, K., Moseley, M. L., Jacobsen, J. F., Kress, W., Naylor, S. L. *et al.* (2001). Myotonic dystrophy type 2 caused by a CCTG expansion in intron 1 of ZNF9. *Science*, **293**, 864–867.
5. Bachinski, L. L., Udd, B., Meola, G., Sansone, V., Bassez, G., Eymard, B. *et al.* (2003). Confirmation of the type 2 myotonic dystrophy (CCTG)n expansion mutation in patients with proximal myotonic myopathy/proximal myotonic dystrophy of different European origins: a single shared haplotype indicates an ancestral founder effect. *Am. J. Hum. Genet.* **73**, 835–848.
6. Liquori, C. L., Ikeda, Y., Weatherspoon, M., Ricker, K., Schoser, B. G., Dalton, J. C. *et al.* (2003). Myotonic dystrophy type 2: human founder haplotype and evolutionary conservation of the repeat tract. *Am. J. Hum. Genet.* **73**, 849–862.
7. Udd, B., Meola, G., Krahe, R., Thornton, C., Ranum, L., Day, J. *et al.* (2003). Report of the 115th ENMC workshop: DM2/PROMM and other myotonic dystrophies. 3rd Workshop, 14-16 February 2003, Naarden, The Netherlands. *Neuromuscul. Disord.* **13**, 589–596.
8. Mankodi, A., Logigian, E., Callahan, L., McClain, C., White, R., Henderson, D. *et al.* (2000). Myotonic dystrophy in transgenic mice expressing an expanded CUG repeat. *Science*, **289**, 1769–1773.
9. Charlet, B., Savkur, R. S., Singh, G., Philips, A. V., Grice, E. A. & Cooper, T. A. (2002). Loss of the muscle-

specific chloride channel in type 1 myotonic dystrophy due to misregulated alternative splicing. *Mol. Cell*, **10**, 45–53.
10. Mankodi, A., Takahashi, M. P., Jiang, H., Beck, C. L., Bowers, W. J., Moxley, R. T. *et al.* (2002). Expanded CUG repeats trigger aberrant splicing of ClC-1 chloride channel pre-mRNA and hyperexcitability of skeletal muscle in myotonic dystrophy. *Mol. Cell*, **10**, 35–44.
11. Mankodi, A., Urbinati, C. R., Yuan, Q. P., Moxley, R. T., Sansone, V., Krym, M. *et al.* (2001). Muscleblind localizes to nuclear foci of aberrant RNA in myotonic dystrophy types 1 and 2. *Hum. Mol. Genet.* **10**, 2165–2170.
12. Kanadia, R. N., Johnstone, K. A., Mankodi, A., Lungu, C., Thornton, C. A., Esson, D. *et al.* (2003). A muscleblind knockout model for myotonic dystrophy. *Science*, **302**, 1978–1980.
13. Lu, X., Timchenko, N. A. & Timchenko, L. T. (1999). Cardiac elav-type RNA-binding protein (ETR-3) binds to RNA CUG repeats expanded in myotonic dystrophy. *Hum. Mol. Genet.* **8**, 53–60.
14. Miller, J. W., Urbinati, C. R., Teng-Umnuay, P., Stenberg, M. G., Byrne, B. J., Thornton, C. A. & Swanson, M. S. (2000). Recruitment of human muscleblind proteins to (CUG)(n) expansions associated with myotonic dystrophy. *EMBO J.* **19**, 4439–4448.
15. Tian, B., White, R. J., Xia, T., Welle, S., Turner, D. H., Mathews, M. B. & Thornton, C. A. (2000). Expanded CUG repeat RNAs form hairpins that activate the double-stranded RNA-dependent protein kinase PKR. *RNA*, **6**, 79–87.
16. Mankodi, A., Teng-Umnuay, P., Krym, M., Henderson, D., Swanson, M. & Thornton, C. A. (2003). Ribonuclear inclusions in skeletal muscle in myotonic dystrophy types 1 and 2. *Ann. Neurol.* **54**, 760–768.
17. Ranum, L. P. & Day, J. W. (2002). Dominantly inherited, non-coding microsatellite expansion disorders. *Curr. Opin. Genet. Dev.* **12**, 266–271.
18. Mahadevan, M. S., Yadava, R. S., Yu, Q., Balijepalli, S., Frenzel-McCardell, C. D., Bourne, T. D. & Phillips, L. H. (2006). Reversible model of RNA toxicity and cardiac conduction defects in myotonic dystrophy. *Nature Genet.* **38**, 1066–1070.
19. Cho, D. H. & Tapscott, S. J. (2006). Myotonic dystrophy: Emerging mechanisms for DM1 and DM2. *Biochim. Biophys. Acta*, **1772**, 195–204.
20. Vihola, A., Bassez, G., Meola, G., Zhang, S., Haapasalo, H., Paetau, A. *et al.* (2003). Histopathological differences of myotonic dystrophy type 1 (DM1) and PROMM/DM2. *Neurology*, **60**, 1854–1857.
21. Ho, T. H., Savkur, R. S., Poulos, M. G., Mancini, M. A., Swanson, M. S. & Cooper, T. A. (2005). Colocalization of muscleblind with RNA foci is separable from misregulation of alternative splicing in myotonic dystrophy. *J. Cell Sci.* **118**, 2923–2933.
22. Flink, I. L. & Morkin, E. (1995). Alternatively processed isoforms of cellular nucleic acid-binding protein interact with a suppressor region of the human beta-myosin heavy chain gene. *J. Biol. Chem.* **270**, 6959–6965.
23. Chen, W., Liang, Y., Deng, W., Shimizu, K., Ashique, A. M., Li, E. & Li, Y. P. (2003). The zinc-finger protein CNBP is required for forebrain formation in the mouse. *Development*, **130**, 1367–1379.
24. Schoser, B. G., Ricker, K., Schneider-Gold, C., Hengstenberg, C., Durre, J., Bultmann, B. *et al.* (2004). Sudden cardiac death in myotonic dystrophy type 2. *Neurology*, **63**, 2402–2404.
25. Schneider-Gold, C., Beer, M., Kostler, H., Buchner, S., Sandstede, J., Hahn, D. & Toyka, K. V. (2004). Cardiac and skeletal muscle involvement in myotonic dystrophy type 2 (DM2): a quantitative 31P-MRS and MRI study. *Muscle Nerve*, **30**, 636–644.
26. Ranum, L. P. & Day, J. W. (2002). Myotonic dystrophy: clinical and molecular parallels between myotonic dystrophy type 1 and type 2. *Curr. Neurol. Neurosci. Rep.* **2**, 465–470.
27. Ranum, L. P. & Day, J. W. (2004). Myotonic dystrophy: RNA pathogenesis comes into focus. *Am. J. Hum. Genet.* **74**, 793–804.
28. Udd, B., Meola, G., Krahe, R., Thornton, C., Ranum, L. P., Bassez, G. *et al.* (2006). 140th ENMC International Workshop: Myotonic Dystrophy DM2/PROMM and other myotonic dystrophies with guidelines on management. *Neuromuscul. Disord.* **16**, 403–413.
29. Klesert, T. R., Cho, D. H., Clark, J. I., Maylie, J., Adelman, J., Snider, L. *et al.* (2000). Mice deficient in Six5 develop cataracts: implications for myotonic dystrophy. *Nature Genet.* **25**, 105–109.
30. Sarkar, P. S., Appukuttan, B., Han, J., Ito, Y., Ai, C., Tsai, W. *et al.* (2000). Heterozygous loss of Six5 in mice is sufficient to cause ocular cataracts. *Nature Genet.* **25**, 110–114.
31. Konicek, B. W., Xia, X., Rajavashisth, T. & Harrington, M. A. (1998). Regulation of mouse colony-stimulating factor-1 gene promoter activity by AP1 and cellular nucleic acid-binding protein. *DNA Cell Biol.* **17**, 799–809.
32. Margolis, J. M., Schoser, B. G., Moseley, M. L., Day, J. W. & Ranum, L. P. (2006). DM2 intronic expansions: evidence for CCUG accumulation without flanking sequence or effects on ZNF9 mRNA processing or protein expression. *Hum. Mol. Genet.* **15**, 1808–1815.
33. Li, Y. P., Chen, W., Liang, Y., Li, E. & Stashenko, P. (1999). Atp6i-deficient mice exhibit severe osteopetrosis due to loss of osteoclast-mediated extracellular acidification. *Nature Genet.* **23**, 447–451.
34. Berul, C. I., Aronovitz, M. J., Wang, P. J. & Mendelsohn, M. E. (1996). In vivo cardiac electrophysiology studies in the mouse. *Circulation*, **94**, 2641–2648.
35. Berul, C. I., Christe, M. E., Aronovitz, M. J., Seidman, C. E., Seidman, J. G. & Mendelsohn, M. E. (1997). Electrophysiological abnormalities and arrhythmias in alpha MHC mutant familial hypertrophic cardiomyopathy mice. *J. Clin. Invest.* **99**, 570–576.
36. Berul, C. I., Christe, M. E., Aronovitz, M. J., Maguire, C. T., Seidman, C. E., Seidman, J. G. & Mendelsohn, M. E. (1998). Familial hypertrophic cardiomyopathy mice display gender differences in electrophysiological abnormalities. *J. Interv. Card. Electrophysiol.* **2**, 7–14.

Edited by J. Karn

(Received 14 December 2006; received in revised form 30 January 2007; accepted 31 January 2007)
Available online 9 February 2007